Supporting Information

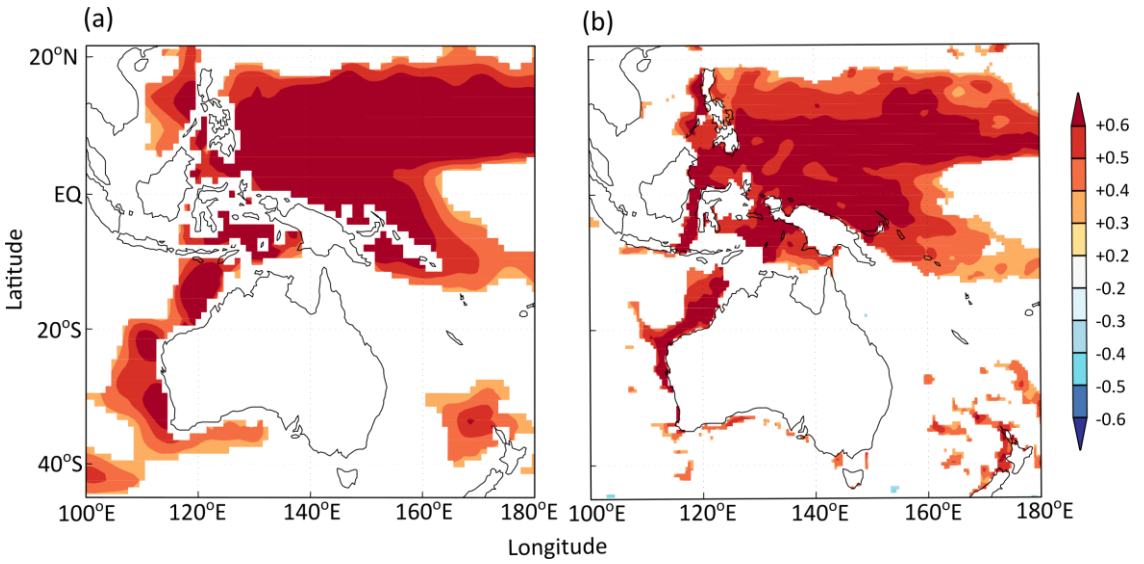

Supplementary Figure S1. Significant correlations ($p < 0.05$) between annual Fremantle sea level and the environmental variables, ocean heat content and ocean mean temperature. Maps show correlations between Fremantle sea level and (a) ocean temperature from 0–700m depth from the years 1969–2008 and (b) ocean heat content from the years 1969–2004. Warmer colours indicate positive correlations, cooler colours indicate negative correlations. Spatial correlation maps were obtained and modified from KNMI Climate Explorer.

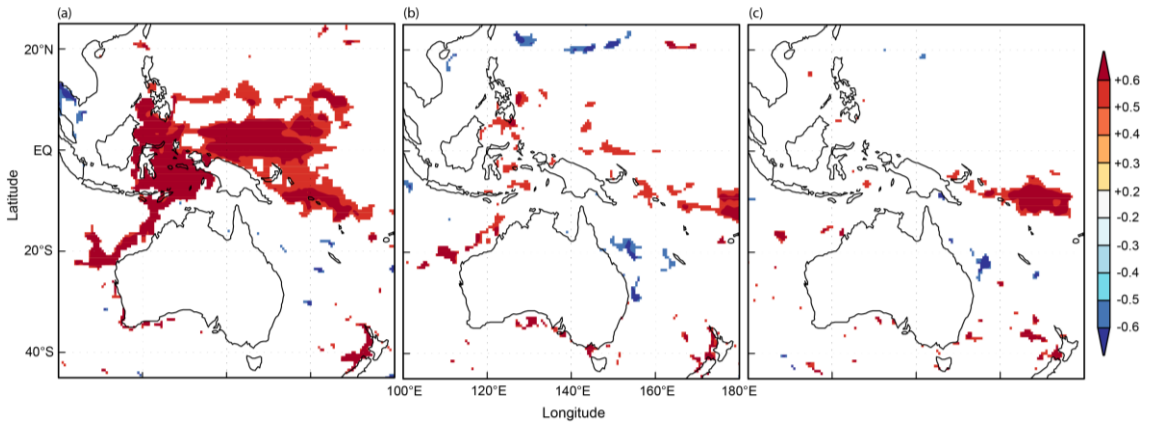

Supplementary Figure S2. Significant correlations ($p < 0.05$) between the first principal component ($PC1_{inv}$) and ocean heat content from 0–750 m depth. $PC1_{inv}$ was constructed from the growth chronologies of six marine fish species in Western Australia and inverse values were used in the map because five out of the six species were negatively loaded on PC1. Maps show correlations between $PC1_{inv}$ with ocean heat content from (a) April to June, (b) July to September and (c) October to December. Warmer colours indicate positive correlations, cooler colours indicate negative correlations. All data were from the years 1988 to 2003 and spatial correlation maps were obtained and modified from KNMI Climate Explorer.

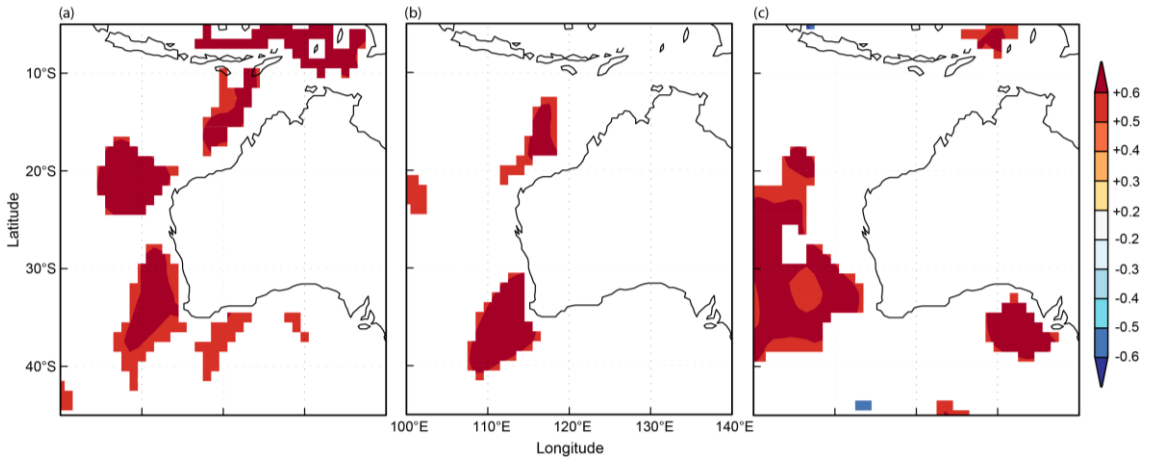

Supplementary Figure S3. Significant correlations ($p < 0.05$) between the first principal component ($PC1_{inv}$) and quarterly ocean temperature from 0–700 m depth. $PC1_{inv}$ was constructed from the growth chronologies of six marine fish species in Western Australia and inverse values were used in the map because five out of the six species were negatively loaded on PC1. Maps show correlations between $PC1_{inv}$ with ocean temperature from (a) April to June, (b) July to September and (c) October to December. Warmer colours indicate positive correlations, cooler colours indicate negative correlations. All data were from the years 1988 to 2003 and spatial correlation maps were obtained and modified from KNMI Climate Explorer.

Supplementary Table S1. Life history characteristics and climatic preferences of six marine fishes. Information collated from fishbase.org for each species, except for the longevity of *Lutjanus argentimaculatus* and *Scorpis aequipinnis*, where the information were taken from Piddocke *et al.* (2015) and Coulson *et al.* (2012), respectively.

Species	Climatic preferences	Depth range in metres from literature (depth range of collected samples in metres)	Trophic level	Longevity (years)	Maximum length (cm)
Lutjanus argentimaculatus	Tropical	1 – 120 (50 –120)	3.6	57	150
Lutjanus bohar	Tropical	4 – 180 (80 –180)	4.3	55	90
Lethrinus nebulosus	Tropical	10 – 75 (5 –80)	3.8	28	87
Scorpis aequipinnis	Temperate	20 – 50 (5 – 50)	3.3	68	48
Achoerodus gouldii	Subtropical to Temperate	6 – 65 (5 – 100)	3.8	70	175
Polyprion oxygeneios	Subtropical to Temperate	50 – 854 (200 – 450)	4.5	60	160

Supplementary Table S2. Summary of the otolith growth chronologies of fish from Western Australia. ENSO = El Niño-Southern Oscillation, SSS = Sea surface salinity, PDO = Pacific Decadal Oscillation, SL = sea level, SST = sea surface temperature. Lag indicates that the growth chronologies were significantly correlated with environmental variables in the previous year. Drivers of growth are those identified in the publications listed.

Species	Length of chronology	Location (sample size)	Publication source (reference)	Drivers of growth
Lutjanus argentimaculatus	1975 – 2004	North Coast, Gascoyne Coast (36)	Ong *et al.*, 2015	ENSO, SSS, PDO
Lutjanus bohar	1962 – 2007	North Coast (55)	Ong *et al.*, 2017	Rainfall, SL, PDO
Lethrinus nebulosus	1980 – 2009	Gascoyne Coast (23)	Ong *et al.*, 2016	SST, Rainfall
Scorpis aequipinnis	1952 – 2009	South Coast (28)	--	--
Achoerodus gouldii	1952 – 2003	South Coast (56)	Rountrey *et al.*, 2014	SST
Polyprion oxygeneios	1979 – 2009	West Coast, South Coast (44)	Nguyen *et al.*, 2015	SL (lag), SST (lag)

Supplementary Table S3. Results of bootstrapped $\bar{r}$ and expressed population signal (EPS) for the detrended and standardized growth chronologies of six marine fishes from Western Australia. The period with synchronous growth signals (synchronous period) was determined using the conditions $\bar{r} > 0$ and EPS > 0.5. The values of $\bar{r}$, 95% confidence interval (CI) for $\bar{r}$ and EPS represent the average values for the chronologies during the period of overlap for all species (1988 to 2003, 16 years).

Species	Synchronous period	$\bar{r}$	95% CI for $\bar{r}$	EPS
Lutjanus argentimaculatus	1975–2004	0.153	0.122–0.182	0.838
Lutjanus bohar	1970–2007	0.090	0.043–0.137	0.768
Lethrinus nebulosus	1981–2006	0.112	0.034–0.184	0.690
Scorpis aequipinnis	1985–2008	0.104	0.074–0.134	0.744
Achoerodus gouldii	1969–2003	0.021	0.007–0.035	0.540
Polyprion oxygeneios	1988–2003	0.030	0.002–0.057	0.553

Supplementary Table S4. Pearson's correlation matrix of the four environmental variables (annual means) over the years 1988 to 2003. SL = sea level, MEI = Multivariate El Niño-Southern Oscillation Index, PDO = Pacific Decadal Oscillation, DMI = Dipole Mode Index.

Variable	MEI	PDO	DMI
Fremantle SL	-0.86	-0.60	-0.21
MEI	–	+0.69	+0.29
PDO	+0.69	–	-0.05
DMI	+0.29	-0.05	–

Image analyses for *Scorpis aequipinnis*

Only those sectioned otoliths of *S. aequipinnis* that had clearly defined opaque zones, which form annually (Coulson *et al.*, 2012), were considered for inclusion in the analyses. These 28 individuals ranged in age from 37–69 years (median = 45.5), including year-classes between 1940 and 1973. Following the methods of Rountrey *et al.* (2014) and using the plugin "IncMeas" (Rountrey, 2009) written for Image J (National Institutes of Health, USA), a polyline transect was drawn on the digital otolith image, dorsal to the sulcus acusticus and parallel to the direction of growth. The earliest two to six increments were excluded because these increments typically had diffuse boundaries that prevented accurate measurements. Visual crossdating was complicated by the very small variations in increment width that were extremely difficult to distinguish by eye. Consequently, we employed COFECHA software (Holmes, 1983) for statistical cross-dating, using the dates of capture to anchor each increment time series, following the methods of Black *et al.* (2005). Statistical cross-dating was used to check the correct assignments of calendar years to increments (Black *et al.*, 2016) and any errors were inspected visually before measurements were changed.

Environmental datasets

Annual mean values of the sea level at Fremantle Port (FSL), a well-known proxy for the strength of the Leeuwin Current (Feng *et al.*, 2003) were obtained from the Bureau of Meteorology (Australian Government) website, http://www.bom.gov.au. Annual means of three climate indices; the multivariate ENSO index (Wolter & Timlin, 1993), Pacific Decadal Oscillation (PDO) based on sea surface temperature (SST) anomalies over the North Pacific (Mantua & Hare, 2002) and the Dipole Mode Index (DMI), the difference in SST anomalies between the western and eastern equatorial Indian Ocean (Saji *et al.*, 1999) were obtained from the Royal Netherlands Meteorological Institute, KNMI Climate Explorer (Trouet & Van Oldenborgh, 2013), a web application for climate data (http://climexp.knmi.nl). These climate indices were chosen because previous studies have found links between ENSO and PDO indices and otolith growth in western Australia (Ong *et al.*, 2015, Ong *et al.*, 2016). In addition, the mode of the Indian Ocean dipole (described by the DMI) affects the amount of austral winter and spring rainfall (Ashok *et al.*, 2003, Cai *et al.*, 2009). Quarterly spatial correlation maps were constructed to show the relationship between growth of adult fish in western Australia and ocean heat content from 0–750 m depth, obtained from the Simple

Ocean Data Assimilation reanalysis of ocean climate variability (Carton & Giese, 2008). This variable was chosen because SST and ocean heat content were previously identified as influencing fish growth in western Australia (Rountrey *et al.*, 2014, Ong *et al.*, 2015, Ong *et al.*, 2016). Quarterly spatial correlation maps were constructed to illustrate the relationship between growth and ocean mean temperatures from 0–700 m depths, obtained from National Oceanic and Atmospheric Administration World Ocean Atlas (Locarnini *et al.*, 2013). All spatial correlation maps were constructed in KNMI Climate Explorer.

References

Ashok, K., Guan, Z., Yamagata, T. (2003) Influence of the Indian Ocean Dipole on the Australian winter rainfall. Geophysical Research Letters, **30**, L1821.

Black, B. A., Boehlert, G. W., Yoklavich, M. M. (2005) Using tree-ring crossdating techniques to validate annual growth increments in long-lived fishes. Canadian Journal of Fisheries and Aquatic Sciences, **62**, 2277-2284.

Black, B. A., Griffin, D., Van Der Sleen, P. *et al.* (2016) The value of crossdating to retain high-frequency variability, climate signals, and extreme events in environmental proxies. Global Change Biology, **22**, 2582-2595.

Cai, W., Cowan, T., Sullivan, A. (2009) Recent unprecedented skewness towards positive Indian Ocean Dipole occurrences and its impact on Australian rainfall. Geophysical Research Letters, **36,** L11705, doi: 10.1029/2009GL037604.

Carton, J. A., Giese, B. S. (2008) A reanalysis of ocean climate using Simple Ocean Data Assimilation (SODA). Monthly Weather Review, **136**, 2999-3017.

Coulson, P. G., Potter, I. C., Hall, N. G. (2012) The biological characteristics of *Scorpis aequipinnis* (Kyphosidae), including relevant comparisons with those of other species and particularly of a heavily exploited congener. Fisheries Research, **125–126**, 272-282.

Feng, M., Meyers, G., Pearce, A., Wijffels, S. (2003) Annual and interannual variations of the Leeuwin Current at 32°S. Journal of Geophysical Research: Oceans, **108**, 3355.

Holmes, R. L. (1983) Computer-assisted quality control in tree-ring dating and measurement. Tree-ring Bulletin, **43**, 69-78.

Locarnini, R. A., Mishonov, A. V., Antonov, J. I. *et al.* (2013) World Ocean Atlas 2013, Volume 1: Temperature. In: *NOAA Atlas NESDIS 73.* (eds Levitus S, Mishonov A) pp Page, NOAA.

Mantua, N. J., Hare, S. R. (2002) The Pacific Decadal Oscillation. Journal of Oceanography, **58**, 35-44.

Nguyen, H. M., Rountrey, A. N., Meeuwig, J. J. *et al.* (2015) Growth of a deep-water, predatory fish is influenced by the productivity of a boundary current system. Scientific Reports, **5**, 9044.

Ong, J. J. L., Rountrey, A. N., Marriott, R. J., Newman, S. J., Meeuwig, J. J., Meekan, M. G. (2017) Cross-continent comparisons reveal differing environmental drivers of growth of the coral reef fish, Lutjanus bohar. Coral Reefs, **36**, 195-206.

Ong, J. J. L., Rountrey, A. N., Meeuwig, J. J., Newman, S. J., Zinke, J., Meekan, M. G. (2015) Contrasting environmental drivers of adult and juvenile growth in a marine fish: implications for the effects of climate change. Scientific Reports, **5,** , 10859.

Ong, J. J. L., Rountrey, A. N., Zinke, J. *et al.* (2016) Evidence for climate-driven synchrony of marine and terrestrial ecosystems in northwest Australia. Global Change Biology, **22**, 2776-2786.

Piddocke, T. P., Butler, G. L., Butcher, P. A., Stewart, J., Bucher, D. J., Christidis, L. (2015) Age and growth of mangrove red snapper Lutjanus argentimaculatus at its cool-water-range limits. Journal of Fish Biology, **86**, 1587-1600.

Rountrey, A. N. (2009) Life histories of juvenile woolly mammoths from Siberia: stable isotope and elemental analyses of tooth dentin. Unpublished Ph.D. thesis PhD Thesis, The University of Michigan, 336 pp.

Rountrey, A. N., Coulson, P. G., Meeuwig, J. J., Meekan, M. G. (2014) Water temperature and fish growth: otoliths predict growth patterns of a marine fish in a changing climate. Global Change Biology, **20**, 2450-2458.

Saji, N. H., Goswami, B. N., Vinayachandran, P. N., Yamagata, T. (1999) A dipole mode in the tropical Indian Ocean. Nature, **401**, 360-363.

Trouet, V., Van Oldenborgh, G. J. (2013) KNMI Climate Explorer: a web-based research tool for high-resolution paleoclimatology. Tree-ring Research, **69**, 3-13.

Wolter, K., Timlin, M. S. (1993) Monitoring ENSO in COADS with a seasonally adjusted principal component index. In: *Proceedings of the 17th Climate Diagnostics Workshop.* pp Page.